DOI: 10.1002/chem.200701333

A General Method for Constructing Optically Active Supramolecular Assemblies from Intrinsically Achiral Water-Insoluble Free-Base Porphyrins

Yiqun Zhang, Penglei Chen,* and Minghua Liu*[a]

Abstract: We have developed a general method to construct optically active porphyrin supramolecular assemblies by using a simple air–water interfacial assembly process. The method involved the in situ diprotonation of the free-base porphyrins at the air–water interface and subsequent assembly under compression. We showed that two intrinsically achiral water-insoluble free-base porphyrin derivatives, 2,3,7,8,12,13,17,18-octaethyl-21*H*,23*H*-porphine (H_2OEP) and 5,10,15,20-tetra-*p*-tolyl-21*H*,23*H*-porphine (H_2TPPMe), could be diprotonated when spread onto a 2.4 M hydrochloric acid solution surface, and the Langmuir–Schaefer (LS) films fabricated from the subphase exhibited strong circular dichroism (CD) absorption, whereas those fabricated from pure Milli-Q water subphase did not. The experimental data suggested that the helical stacking of the achiral porphyrin building blocks was responsible for the supramolecular chirality of the assemblies. Interestingly, such a method was successfully applied to a series of other intrinsically achiral free-base porphyrins such as 5,10,15,20-tetrakis(4-methoxyphenyl)-21*H*,23*H*-porphine (H_2TPPOMe), 5,10,15,20-tetraphenyl-21*H*,23*H*-porphine (H_2TPP), 5,10,15,20-tetrakis(4-(allyloxy)phenyl)-21*H*,23*H*-porphine (H_2TPPOA), and 5,10,15,20-tetrakis(3,5-dimethoxyphenyl)-21*H*,23*H*-porphine (H_2TPPDOMe). A possible mechanism has been proposed. The method provides a facile way to obtain optically active porphyrin supramolecular assemblies by using intrinsically achiral water-insoluble free-base porphyrin derivatives.

Keywords: porphyrinoids · supramolecular assemblies · symmetry breaking · thin films

Introduction

Chirality, which displays itself in various forms and occurs at all length scales throughout nature, ranging from molecular level to supramolecular level, and from microscopic to macroscopic length scale, is intimately related to the sophisticated biological activities that occur in living systems.[1] The construction of optically active supramolecular assemblies, which are generally linked through noncovalent interactions such as π–π stacking, hydrogen bonds, electrostatic interaction, coordination, and hydrophobic interaction, is one of the most significant issues both in biosupramolecular chemistry and material sciences, owing to the potent abilities of the assemblies to imitate biomacromolecules, as well as potential applications of these systems for developing enantioselective and/or chemical sensors, catalysts, liquid crystals, chiroptical devices, and others.[2]

Porphyrin derivatives have been recognized to be one of the most distinguished building blocks for constructing supramolecular assemblies, owing to their fully understood unique geometric structures, and the characteristic and readily tunable spectroscopic properties.[3] Moreover, their intrinsic and strong ability to mimic the biological processes such as photosynthesis makes them important models for obtaining detailed insights into the operation of antenna systems occurring in green plants in nature.[4] Various artificial photoelectronic systems based on chiral porphyrin supramolecular assemblies are anticipated to be potentially useful for practical applications in the fields of nonlinear optics, material and polymer sciences, catalysis, biochemistry, and molecular devices.[3a–d,4,5] Driven by these factors, supramolecular chirality generation/induction (termed supramolecular chirogenesis), amplification, and memory derived from porphyrin derivatives have currently become some of the hottest topics in the interdisciplinary area of supramolecular chemistry/chirality.[3k] Generally, there are several ways to fabricate optically active porphyrin supramolecular

[a] Y. Zhang, Dr. P. Chen, Prof. Dr. M. Liu
Beijing National Laboratory for Molecular Science
CAS Key Laboratory of Colloid, Interface and Chemical Thermodynamics
Institute of Chemistry, Chinese Academy of Sciences
Beijing 100080 (China)
Fax: (+86) 10-6256-9564
E-mail: chenpl@iccas.ac.cn
liumh@iccas.ac.cn

assemblies: i) from intrinsically chiral porphyrin molecules bearing chiral substituents that have assembled through covalent bonds or noncovalent intermolecular interactions;[4,6] ii) from achiral porphyrin components that have assembled in a chiral circumstance, or were induced by chiral inducers or chiral templates;[3,7] iii) entirely from achiral porphyrin molecules through the asymmetric outer-vortex motion, or directional spin coating.[8,9] The third case is thought to be very important, because it relates to the origin of supramolecular chirality and the symmetry breaking of a system.

We have recently found that Langmuir, as well as Langmuir–Schaefer (LS) techniques, appeared to be very effective in obtaining chiral molecular assemblies from achiral building blocks.[10,11] Herein, we describe how we have established a general way to obtain chiral porphyrin assemblies from achiral porphyrins through interfacial assembly. The method involves the in situ diprotonation of the porphyrins at the air–water interface and subsequent assembly under compression. We found that two water-insoluble free-base intrinsically achiral porphyrin derivatives, 2,3,7,8,12,13,17,18-octaethyl-21*H*,23*H*-porphine (H_2OEP) and 5,10,15,20-tetra-*p*-tolyl-21*H*,23*H*-porphine (H_2TPPMe), could be diprotonated when spread on a hydrochloric acid solution surface, and the LS films fabricated from this subphase exhibited strong circular dichroism (CD), whereas films fabricated at a Milli-Q water surface did not. Such a method was successfully applied to a series of other free-base porphyrins such as 5,10,15,20-tetrakis(4-methoxyphenyl)-21*H*,23*H*-porphine (H_2TPPOMe), 5,10,15,20-tetraphenyl-21*H*,23*H*-porphine (H_2TPP), 5,10,15,20-tetrakis(4-(allyloxy)phenyl)-21*H*,23*H*-porphine (H_2TPPOA), and 5,10,15,20-tetrakis(3,5-dimethoxyphenyl)-21*H*,23*H*-porphine (H_2TPPDOMe). The method is universal and optically active assemblies were successfully obtained from all of the achiral porphyrins shown in Scheme 1. The methodology describes a potentially simple and general way of synthesizing optically active porphyrin supramolecular assemblies by using water-insoluble achiral porphyrin building blocks.

Results and Discussion

Surface pressure–molecular area isotherms of the Langmuir films of H_2OEP and H_2TPPMe: Figure 1 shows the surface pressure–molecular area isotherms of H_2OEP and H_2TPPMe on a pure Milli-Q water surface and those on a 2.4 M hydrochloric acid subphase at 20 °C.[12] The limiting areas per molecule on pure Milli-Q water subphase were 0.1 and 0.38 nm^2, for H_2OEP and H_2TPPMe, respectively. The onset of the surface pressure was observed at 0.14 and 0.44 nm^2 molecule^{-1} for H_2OEP and H_2TPPMe, respectively. These values were much smaller than the corresponding theoretical values calculated by the Corey–Pauling–Koltun (CPK) model, indicating the possible existence of substantial aggregations on the water surface. The limiting areas per molecule obtained on a 2.4 M hydrochloric acid subphase were 0.58 and 0.87 nm^2, for H_2OEP and H_2TPPMe, respectively. The onset of the surface pressure was observed at 0.73 and at 1.61 nm^2 molecule^{-1} for H_2OEP and for H_2TPPMe, respectively. These data were apparently larger than those calculated for the Milli-Q water surface. The collapsed surface pressure decreased dramatically when using the hydrochloric acid subphase compared with those for the pure Milli-Q water surface, suggesting the intermolecular π–π interactions were weakened to some extent when hydrochloric acid was employed as the subphase. These changes indicated that a more expanded spreading film was obtained when hydrochloric acid was used as the subphase, where the type of molecular packing differed from that obtained on the pure Milli-Q water surface.

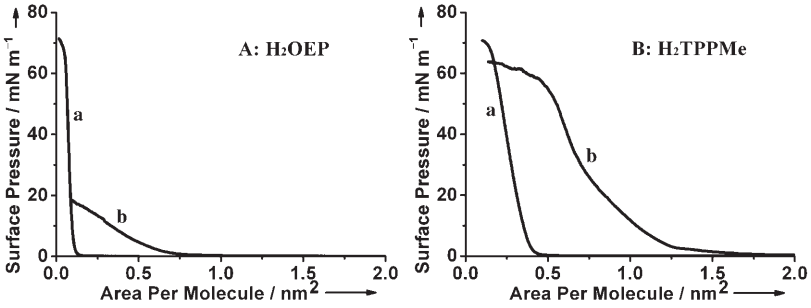

Figure 1. Surface pressure–molecular area isotherms of: (A) H_2OEP and; (B) H_2TPPMe on: (a) Pure Milli-Q surface and (b) The 2.4 M hydrochloric acid subphase, at 20 °C.

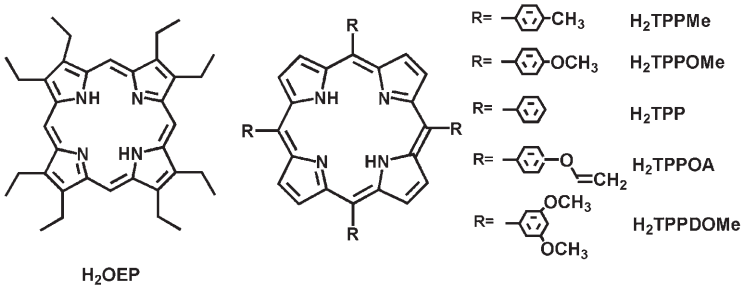

Scheme 1. The chemical structure of the achiral water-insoluble free-base porphyrins investigated.

UV/Vis spectra of H_2OEP and H_2TPPMe in solution and LS films: Figure 2 shows the UV/Vis spectra of the LS films and those in the corresponding solutions in chloroform. The UV/Vis solution spectra of H_2OEP in chloroform exhibited a Soret band at 400 nm, and four Q bands at 498, 534, 566, and 620 nm. Acidified in solution in chloroform, the Soret band red-shifted to 419 nm, and the Q bands exhibited two absorptions at 557 and 598 nm, indicating the diprotonation of the central nitrogen atoms of H_2OEP molecules, which resulted in the formation of the dicationic H_4OEP^{2+} species.[13–17] A broad Soret band centered at 408 nm, and four Q bands at 520, 547, 574, and 629 nm, which were red-shifted compared with those in solution in chloroform, were observed from LS films deposited from the Milli-Q water surface. Based on the exciton coupling model proposed by Kasha and co-workers,[18] it is widely acknowledged that the bathochromic and hypsochromic shifts of the Soret band of porphyrins correspond to the J aggregates and H aggregates, respectively. In the present case, the Soret band was displayed as a broad band. Accordingly, we suggested that the H_2OEP molecules are arranged in various J-type and H-type aggregation species in the LS film when pure Milli-Q water was employed as subphase. The LS film deposited from the hydrochloric acid subphase showed a broad Soret band centered at 402 nm and two Q bands at 548 and 596 nm, which were blue-shifted compared with those in acidified chloroform, similarly indicating that the cationic H_4OEP^{2+} species were arranged in various J-type and H-type aggregations in the as-prepared LS film.[18] In the case of H_2TPPMe, its solution in chloroform shows a Soret band at 420 nm and four Q bands in the region of 500–700 nm. In acidified chloroform solution, a bathochromic-shifted Soret band maximum at 448 nm, and two Q bands at 618 and 672 nm, were observed, similarly indicating the diprotonation of the central nitrogen atoms of H_2TPPMe molecule and the formation of cationic H_4TPPMe^{2+} species.[13–17] The LS film deposited from the pure Milli-Q water subphase shows a Soret band at 438 nm, which is red-shifted by 18 nm with respect to that of the monomeric species in solution, and slight red-shifts are also observed from the Q band, indicating that most of the H_2TPPMe molecules were arranged as J-type aggregates in the as-formulated LS film. The LS film of H_2TPPMe deposited from the 2.4 M hydrochloric acid surface shows a Soret band at 459 nm and two Q bands at 636 and 695 nm, also indicating the diprotonation of the H_2TPPMe molecule center when hydrochloric acid was employed as subphase. Its Soret band also shows distinct red shifts with respect to that of the monomeric molecules in acidified chloroform, similarly indicating that most of the cationic H_4TPPMe^{2+} species formed J-type aggregates.

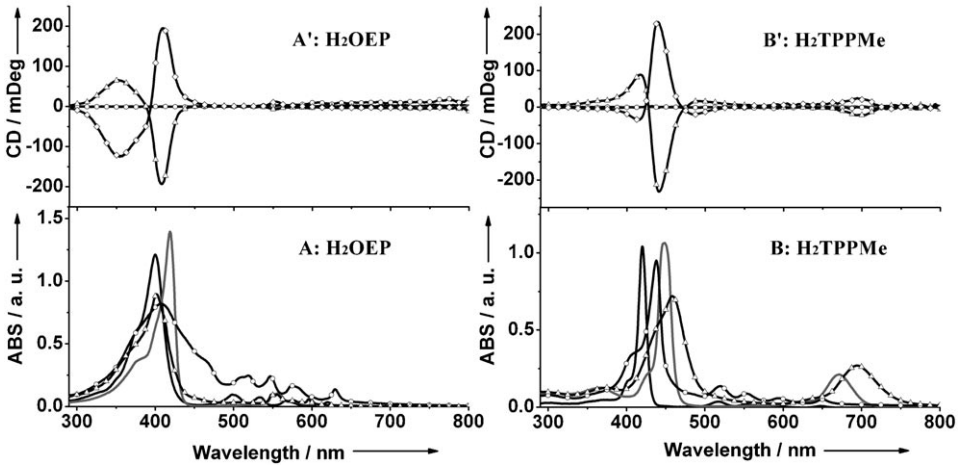

Figure 2. UV/Vis (A and B) and CD (A′ and B′) spectra of H_2OEP (A and A′) and H_2TPPMe (B and B′) in chloroform solution (black), acidified chloroform solution (gray), 20-layer LS films deposited by using pure Milli-Q water (○) and 2.4 M hydrochloric acid (△ and ◇) as subphases. The (△) and (◇) curves were obtained from the LS films deposited in different batches. For H_2OEP, the LS films were deposited at 7 mN m^{-1}, and those of H_2TPPMe were deposited at 30 mN m^{-1}.

CD spectra of H_2OEP and H_2TPPMe in solution and LS films: As indicated in Figure 2, no CD signal was observed for the chloroform and acidified chloroform solutions, and for the LS films of H_2OEP and H_2TPPMe deposited from the Milli-Q water subphase. However, strong CD signals were observed for the LS films deposited from the hydrochloric acid subphase for both of the porphyrins. In the case of H_2OEP, its LS film deposited from the 2.4 M hydrochloric acid subphase exhibited strong bisignated Cotton effect (CE) maxima at 411 and 351 nm, with a crossover at 387 nm, and a monosignated CE maximum at 553 nm, which could mainly be attributed to the contributions provided by Soret and Q bands of the diprotonated species of H_2OEP exhibited by the LS film, respectively, suggesting that strong exciton coupling existed between the porphyrin chromophores due to the H aggregation. For H_2TPPMe, its LS film displayed CE maxima at 416, 438, and 486 nm accompanied by two crossovers at 425 and 469 nm, and a monosignated CE maximum at 694 nm, which could mainly be ascribed to the contributions provided by Soret and Q bands of the diprotonated species of H_2TPPMe displayed by the LS film, respectively. This pattern of splitting CE suggested the existence of exciton coupling between the porphyrin chromophores due to the aggregation of the acidified species of these porphyrins.

It should be noted that the CD signals could be opposite for the LS films deposited in the different batches in most cases, as shown in Figure 2, and occasionally opposite CD

signals could be detected from different regions of the LS film deposited in the same batch. These facts confirmed that the observed chirality was indeed not from any chiral impurities but from the helical-sense assemblies of the building blocks, where the achiral molecules were cooperatively stacked in a helical-sense conformation. This phenomenon is essentially the same as that reported for the chirality of the assemblies obtained from achiral building blocks, which could be due to symmetry breaking.[8–11,19]

Authenticity of the observed macroscopic chirality: It has been suggested that the authenticity of the observed chirality through conventional CD measurement could not be exclusively determined for solid-state samples, because the detected CD spectra are often accompanied by artifacts which usually originate from the interaction between the macroscopic anisotropies of a sample such as birefringence and linear dichroism (LD).[20] Effective strategies for the CD measurement of thin solid films have been proposed by Spitz and co-workers,[21] and used by us previously,[10,11] to validate the authenticity of the chirality detected from the LB or LS films. This can be achieved in two ways. One method is measuring the CD spectra of the sample discontinuously at a certain angle by rotating the film step by step within the film plane. During the measurements, the LS films were discreetly placed perpendicularly to the light path, to exclude the contributions from birefringence. The angle dependence of the amplitude was determined by the difference between the maximum and minimum value, and that of the background was determined by the difference between the values at the upper wavelength and lower edges. Thus an angle dependence behavior of 36 CD spectra, which were measured in a step of 10° around the optical axis, could be determined. The other method to achieve this involves measuring the CD spectra by continuously rotating the sample during the measurement. If the sample intrinsically had genuine chirality, both the methods would give the same results.[10,11]

We measured the CD spectra of the LS film of H_2OEP deposited from the hydrochloric acid subphase according to the above-described methods as an example to illustrate the authenticity of the observed macroscopic chirality. As shown in Figure 3A, the angle dependence of the CD amplitude was determined by the difference between the maximum value at 351 nm and minimum value at 411 nm, and the corresponding angle dependence of the background was determined by the difference between the values at the lower edge at 250 nm and upper wavelength edge at 600 nm, which are displayed as filled squares and circles, respectively. In the case of angle dependence of the background, the observed differences between the values at the upper wavelength and lower edges fluctuated around zero millidegrees, whereas that of the amplitude, exhibited a cosine function, fluctuated around 280 millidegrees, which was positively shifted about 280 millidegrees compared with that of the background. These results suggested the presence of distortion by LD, the film, however, indeed had intrinsic chirality.[21] On the other hand, the CD spectra of the same sample measured by continuously rotating the film during the measurement (Figure 3B), also indicated an approximately 280-millidegree difference between the maximum value at 351 nm and minimum value at 411 nm, which was the same as that after averaging 36 spectra measured at various angles. These results suggested that our LS films indeed have intrinsic macroscopic chirality, which resulted from the helical-sense conformation of the supramolecular assemblies, and that the second method was convenient to measure the CD spectra of thin solid films. As indicated in the Experimental Section, all the CD spectral measurements for the LS films were carried out by the second method.

AFM images of the LS films of H_2OEP and H_2TPPMe: The AFM images of the monolayer LS films of H_2OEP deposited from Milli-Q water and hydrochloric acid subphases are shown in Figure 4. When Milli-Q water was used as a subphase, irregular nanoparticles were observed, owing to the serious aggregation of H_2OEP, as suggested by the π–A isotherm. Interestingly, the same helical-sense nanorods were observed for the film deposited from a certain batch, whereas nanorods with the opposite helical sense (right- or left-handed conformation) could be observed for the films deposited from different batches. Occasionally, both right- and left-handed helical nanorods could be found in the same LS film deposited in the same batch. The width of the nanorods was 70–120 nm, and the helical pitch was about 40 nm, which was significantly larger than the molecular dimension, indicating the formation of supercoils formed by the twisting of the supramolecular assemblies.[22] H_2TPPMe displayed features similar to those shown by H_2OEP (Figure 5). When pure Milli-Q water was used as the subphase, nanoparticles

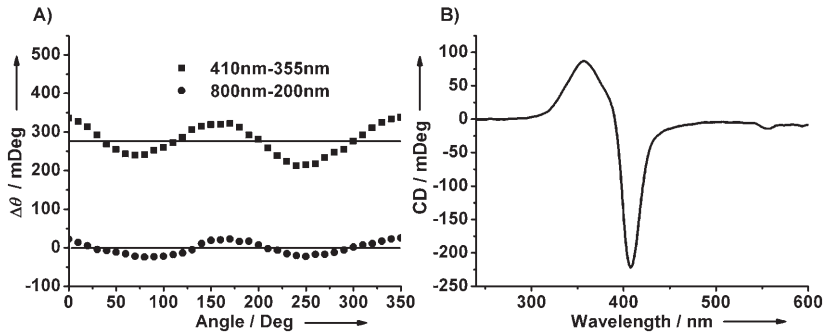

Figure 3. A) Angle dependence of the CD amplitude (■) and the background (●) of the CD spectra of a 20-layer LS film of H_2OEP, which was deposited from 2.4 M hydrochloric acid subphase at 7 $mN\,m^{-1}$. The film was turned around the optical axis in a step of 10° within the sample plane. B) The CD spectrum measured by continuously rotating the sample within its plane.

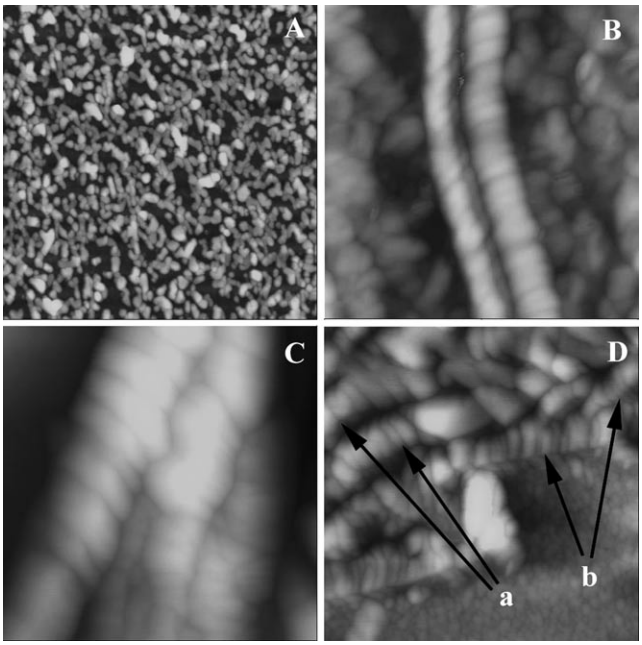

Figure 4. AFM images of monolayer LS films of H_2OEP deposited from pure Milli-Q water (A) and 2.4 M hydrochloric acid subphases (B, C, and D). B and C are the LS films deposited in different batches, where right- (B) and left-handed (C) helical assemblies could be observed. D) Both right- (a) and left-handed (b) helical nanorods could be occasionally found in the different regions of the LS film deposited in the same batch. The scan area was $2\times2\ \mu m^2$ for A, $500\times500\ nm^2$ for B and C, and $750\times750\ nm^2$ for D. The LS films were deposited at $7\ mN\,m^{-1}$.

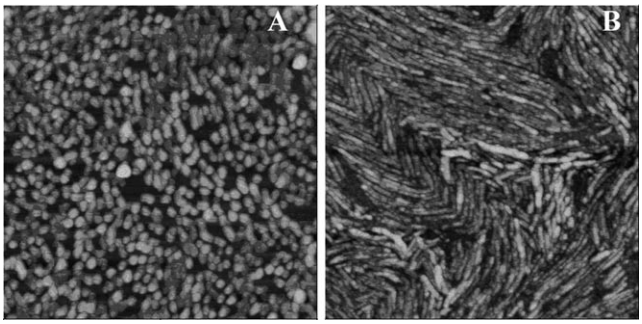

Figure 5. AFM images of monolayer LS films of H_2TPPMe deposited from Milli-Q water (A) and 2.4 M hydrochloric acid subphases (B). The scan area was $2\times2\ \mu m^2$ for all the cases. The LS films were deposited at $30\ mN\,m^{-1}$.

that were arranged in a disordered way were observed, whereas nanorods were detected when hydrochloric acid was employed as the subphase. Although no distinct helical structure could be observed from these nanorods, their CD spectra strongly suggested that the H_2TPPMe molecules were aligned in a helical-sense conformation.

A possible mechanism for formation of the optically active supramolecular assemblies of H_2OEP and H_2TPPMe: Based on the above results, a possible formation mechanism for the macroscopic optical activities of the LS films of H_2OEP was proposed (Figure 6). When pure Milli-Q water was used as the subphase, significant aggregation could occur, owing to the planarity[14b,23] and non-amphiphilicity of the H_2OEP molecules. When the H_2OEP molecules were assembled at the hydrophilic water surface under compression, the strong π–π interaction (resulting from the planarity of H_2OEP) between the porphyrin cores, accompanied by the hydrophobic interactions derived from the ethyl groups, would produce assemblies in which the molecules were tightly arranged as non-specific J-type aggregates. Thus the symmetry breaking essentially had no chance to occur and was almost forbidden, resulting in the LS films showing no macroscopic optical activity. When hydrochloric acid was employed as the subphase, H_2OEP was diprotonated to form the cationic H_4OEP^{2+} species. The diprotonation endowed the neutral H_2OEP molecules with amphiphilicity, which made it a more desirable Langmuir-film-forming material. At the same time, it is known that the diprotonation of the porphyrin center could cause a slight deformation of the porphyrin macrocyclic plane, resulting in a nonplanar (saddle) conformation.[13,14,15a,24] On the other hand, it has been suggested that in the diprotonated cationic porphyrin species, two chloride ions were combined in a near-symmetrical manner above and below the porphyrin macrocyclces by two hydrogen bonds.[16b,25] The larger limiting molecular area per molecule and the greater onset of the surface pressure obtained on the hydrochloric acid subphase compared with those obtained on the pure Milli-Q water surface thus could be partly due to the attachment of the chloride ions on both sides of the porphyrin macrocycles, and partly due to the nonideal planarity of the porphyrin core, which would produce additional spaces and steric hindrance between the neighboring molecules. Due to the steric hindrance brought about by these factors, the intermolecular π–π interactions between the neighboring H_2OEP species could be reduced (as suggested by the π–A isotherms) to some extent and thus it was easier for the H_2OEP molecules to adopt a staggered arrangement with a directional staggering angle, which could promote the occurrence of symmetry breaking. Thus, helical-sense supramolecular assemblies showing mac-

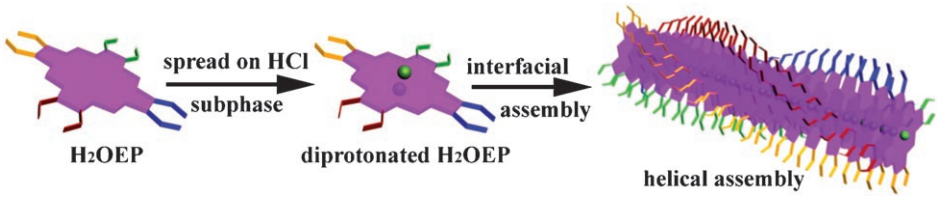

Figure 6. A possible explanation for the interfacially assembled optically active supramolecular assemblies with a helical conformation from H_2OEP by using 2.4 M hydrochloric acid as subphase. The green balls represent axial hydrogen-bonded chloride ions attached on both sides of the porphyrin plane. The slight deformation (saddle) of porphyrin core upon diprotonation was omitted and different colors were employed for clarity.

roscopic optical activities have emerged. The hydrophobic interactions between the beta-positioned ethyl groups together with the cooperative interaction of the weakened π–π interactions between the porphyrin cores caused the formation of H-type aggregates at the 2.4 M hydrochloric acid–air interface upon compression.

In the case of H_2TPPMe, something similar might have happened except that the diprotonated H_2TPPMe molecules were arranged in J-aggregates (scheme not shown). That is, the symmetry breaking was almost forbidden when the nonamphiphilic neutral H_2TPPMe molecules were assembled on the hydrophilic pure Milli-Q water surface under compression, due to the strong intermolecular π–π interactions, resulting in optically inactive LS films. When H_2TPPMe was spread onto the hydrochloric acid subphase, the compound could be diprotonated, which conferred amphiphilicity to the molecule. The steric hindrance, partially brought about by the axial hydrogen-bonded chloride ions on both sides of the porphyrin plane, and partially brought about by the nonideal planarity of the porphyrin core, which resulted from the diprotonation of the porphyrin core, weakened the intermolecular π–π stacking to some extent and provided more opportunities for the symmetry breaking to occur. Additionally, it has been proven that besides the deformation (saddle) of the porphyrin core, the diprotonation could also cause a structural transformation where the free-base porphyrin is converted from a configuration in which the aryl moiety is twisted relative to the mean macrocycle plane to the one in which it is nearly coplanar with the porphyrin core.[17b] Such rotation of the aryl moiety induced by distortion of the macrocycle resulted in an increased aryl ring–porphyrin conjugation.[13,15a,17b,24] Consequently, these factors might be the main driving force to ensure the association of the supramolecular assemblies at the hydrochloric acid surface upon compression, although the intermolecular π–π interaction was weakened to some extent by the distortion of the porphyrin core, and by the axial chloride ions attached by hydrogen bonds on both sides of the porphyrin plane. As a result, the cooperative effect of these two opposite factors (one in favor of, and one against the supramolecular association), accompanied by the interfacial compression, promoted the occurrence of the symmetry breaking and produced the LS films showing macroscopic chirality.

Applicability to other achiral water-insoluble free-base porphyrin derivatives: It can be seen that the above method is an extremely easy way to produce optically active supramolecular assemblies from achiral porphyrins H_2OEP and H_2TPPMe, which is based on a simple mechanism. Thus, it is logical to question whether the method could be suitable for other water-insoluble free-base porphyrins. To examine this, we applied a similar process to four other water-insoluble free-base porphyrins, 5,10,15,20-tetrakis(4-methoxyphenyl)-21*H*,23*H*-porphine (H_2TPPOMe), 5,10,15,20-tetraphenyl-21*H*,23*H*-porphine (H_2TPP), 5,10,15,20-tetrakis(4-(allyloxy)-phenyl)-21*H*,23*H*-porphine (H_2TPPOA), and 5,10,15,20-tetrakis(3,5-dimethoxyphenyl)-21*H*,23*H*-porphine (H_2TPPDOMe), the structures of which are shown in Scheme 1.

As shown in Figure 7 and summarized in Table 1, the limiting molecular areas deduced from the pure Milli-Q water subphase were 0.63, 0.15, 0.61, and 0.70 nm^2 for H_2TPPOMe, H_2TPP, H_2TPPOA, and H_2TPPDOMe, respectively. When hydrochloric acid was employed as the subphase, the corresponding data were 0.87, 0.83, 0.88, and 0.92 nm^2 for the corresponding compounds, which were distinctly larger than those obtained in the former case. The onset of the surface pressures observed from the pure Milli-Q water subphase were evidently smaller than those observed from the 2.4 M hydrochloric acid surface. The collapsed surface pressure also decreased distinctly on the hydrochloric acid subphase compared with that on the pure Milli-Q water surface for all of these four compounds, suggesting the intermolecular π–π interactions were much weaker when hydrochloric acid was employed as the subphase. These changes confirmed that the steric hindrance, partially resulting from the axial chloride ions attached by hydrogen bonds on both sides of the porphyrin plane, and partially resulting from the nonideal planarity of the porphyrin core, which was due to the diprotonation of the porphy-

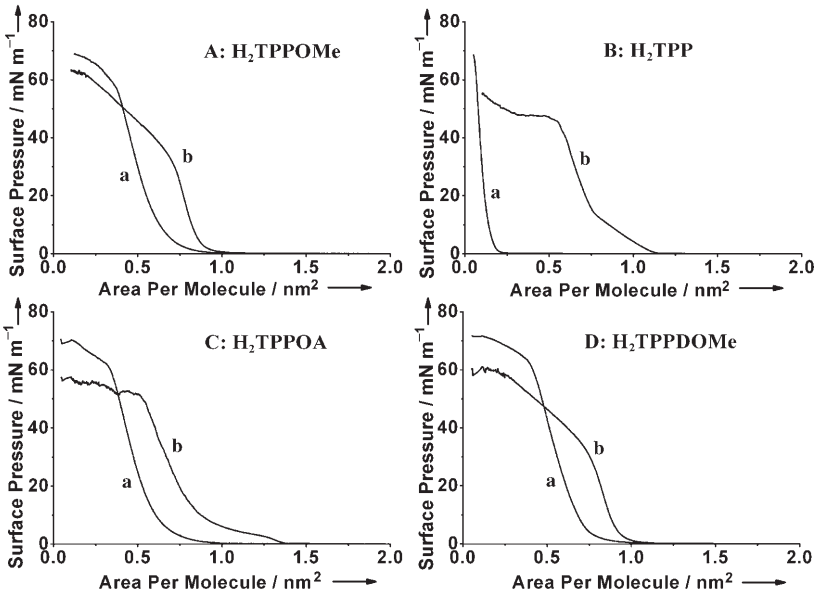

Figure 7. Surface pressure–molecular area (π–A) isotherms of H_2TPPOMe (A), H_2TPP (B), H_2TPPOA (C), and H_2TPPDOMe (D) on pure Milli-Q (a) and 2.4 M hydrochloric acid subphase (b), at 20 °C.

Table 1. Summary of the limiting areas per molecule, and absorption maxima in UV/Vis, CD, and g factor spectra of the investigated porphyrins.

Porphyrin	Samples	Limiting areas per molecule [nm^2]	UV/Vis spectra [nm]		CE maximum [nm]		Maximum magnitude of the g factor at the Soret band [$\times 10^{-3}$]
			Soret band	Q band	Soret band	Q band	
H_2OEP	chloroform		400	498, 534, 566, 620			
	acidified chloroform		419	557, 598			
	LS film (Milli-Q water subphase)	0.1	408	520, 547, 574, 629			
	LS film (2.4 M HCl subphase)	0.58	402	548, 596	351, 411	553	2.5
H_2TPPMe	chloroform		420	518, 553, 592, 648			
	acidified chloroform		448	618, 672			
	LS film (Milli-Q water subphase)	0.38	438	520, 553, 594, 50			
	LS film (2.4 M HCl subphase)	0.87	459	636, 695	416, 438, 486	694	3.1
H_2TPPOMe	chloroform solution		420	519, 556, 594, 650			
	acidified chloroform		452	633, 690			
	LS film (Milli-Q water subphase)	0.63	448	526, 561, 598, 655			
	LS film (2.4 M HCl subphase)	0.87	453	658, 717	420, 459, 506	711	5.2
H_2TPP	chloroform		418	515, 550, 590, 645			
	acidified chloroform		445	610, 661			
	LS film (Milli-Q water subphase)	0.15	441	522, 556, 594, 650			
	LS film (2.4 M HCl subphase)	0.83	465	638, 698	436, 465, 499	691	2.1
H_2TPPOA	chloroform		419	516, 553, 592, 649			
	acidified chloroform		454	633, 689			
	LS film (Milli-Q water subphase)	0.61	444	526, 562, 598, 655			
	LS film (2.4 M HCl subphase)	0.88	449	660, 716	414, 449, 503	716	3.5
H_2TPPDOMe	chloroform		422	516, 550, 589, 648			
	acidified chloroform		458	607, 660			
	LS film (Milli-Q water subphase)	0.70	434	517, 547, 592, 652			
	LS film (2.4 M HCl subphase)	0.92	427	626, 672	397, 445, 537	669	7.5

rin core, could really bring additional spaces and reduce the intermolecular π–π interactions between the neighboring building blocks, and thus affect the packing of the porphyrin building blocks.

The UV/Vis and CD spectra of the other four porphyrins in chloroform, acidified chloroform, and in LS films deposited by using pure Milli-Q water and 2.4 M hydrochloric acid as subphases are presented in Figure 8. A summary of these spectra is collected in Table 1. It can be seen that these four porphyrins could also be diprotonated on the hydrochloric acid subphase. The optical activity properties of the LS films of these four porphyrin derivatives deposited from pure Milli-Q water and hydrochloric acid subphases were also investigated by using CD spectral measurements. The unacidified, acidified chloroform solutions of these compounds showed no CD absorptions, which is similar to what we observed for H_2OEP and H_2TPPMe. For the LS film deposited from the pure Milli-Q water subphase, no CD signal could be observed for the LS films of H_2TPP, H_2TPPOA, and H_2TPPDOMe, and only negligible CD absorption could be observed for the LS films of H_2TPPOMe.[10a] As we have predicted by the mechanism proposed above, all of the LS films of these porphyrin building blocks deposited from the hydrochloric acid subphases show widely split Cotton effects around 340–560 and monosignated Cotton effects around 650–750 nm, which could mainly be assigned to the Soret and Q bands of the diprotonated species of the corresponding compounds, respectively. Crossovers were also observed in the CD curves. Similarly, opposite CD absorptions could be stochastically achieved from the LS film transferred from the different batches in most of the cases, and occasionally opposite CD signals could be detected from different regions of the LS film deposited in the same batch in some rare cases. This is essentially the same as what we have found for H_2OEP and H_2TPPMe, suggesting that the achiral porphyrin building blocks were arranged in helical-sense supramolecular assemblies, and confirming the validity of the proposed mechanism described above.

The AFM images of these four compounds deposited by using pure Milli-Q water and hydrochloric acid as the subphases were also investigated (Figure 9). For the LS films deposited from Milli-Q water, irregular nanoparticles were observed, whereas nanorods with only blurry helical-sense conformations were observed for the LS films deposited hydrochloric acid subphase. These results were the same as those we found for H_2TPPMe. Accordingly, it was reasonable to speculate that these achiral porphyrin building blocks were essentially arranged in helical-structured supramolecular assemblies.

It should be noted that when these porphyrin derivatives were pre-diprotonated in chloroform, they would also form chiral assemblies on the 2.4 M hydrochloric acid subphase. However, when the pre-diprotonated species were spread on the pure Milli-Q water surface, they returned to their free-base form and no chiral assemblies could be obtained. On the other hand, if we transferred the free-base porphyrins spread on the Milli-Q water surface to solid substrates and then acidified the species by exposing the film to moist hydrochloric acid gas, no CD signals were obtained for the assemblies, although the porphyrin could be diprotonated. It

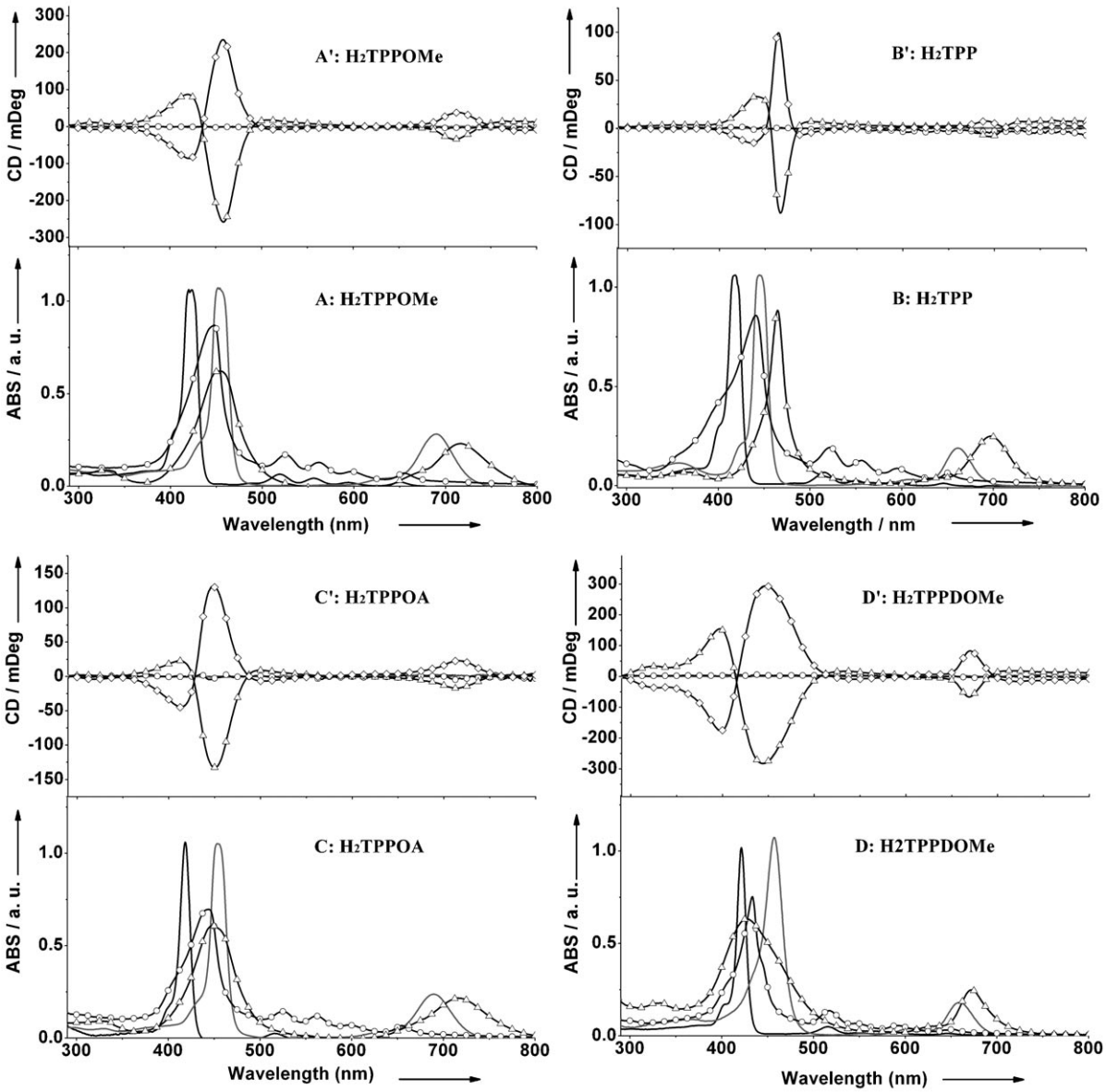

Figure 8. UV/Vis (A, B, C, and D) and CD (A′, B′, C′, and D′) spectra of H_2TPPOMe (A and A′), H_2TPP (B and B′), H_2TPPOA (C and C′), and H_2TPPDOMe (D and D′) in chloroform (black), acidified chloroform (gray), 20-layer LS films deposited by using pure Milli-Q water (○) and 2.4 M hydrochloric acid (△ and ◇) as subphases. The (△) and (◇) curves were obtained from the LS films deposited in different batches. All the LS films were transferred at 30 mN m^{-1} at 20 °C.

seems that the interfacial organization of the diprotonated species is a precondition for obtaining the chiral assemblies from these achiral porphyrins.

A comparison of the macroscopic chirality of LS films by using the g factor: Commonly, accurate knowledge concerning the concentration and cuvette path length of the sample is required for the estimation of CD spectra in terms of the types and amounts of the chiral structures.[26a] For a thin solid film, the definitions of concentration and cuvette path length required for the quantification and analysis of CD data, however, are not clear.[26b] It has recently been suggested that good estimates of the amount of the chiral structures could be obtained from the CD spectra for thin solid films by analyzing the wavelength dependence of the Kuhn g factor, which is also known as the dissymmetry or anisotropy factor, and is defined as the ratio of the CD and UV/Visible absorbance signals of a sample.[26] To make a general comparison of the different optical activity of the LS films formed by different porphyrin derivatives, the g factor spectra of the LS films transferred from the hydrochloric acid subphase, were investigated. Because the g factor spectra of a certain porphyrin derivative generally have an approximately similar profile as those of the corresponding CD spectra shown in Figures 2 and 8, we herein take the g factor spectra of H_2TPPMe as an example for clarity, as

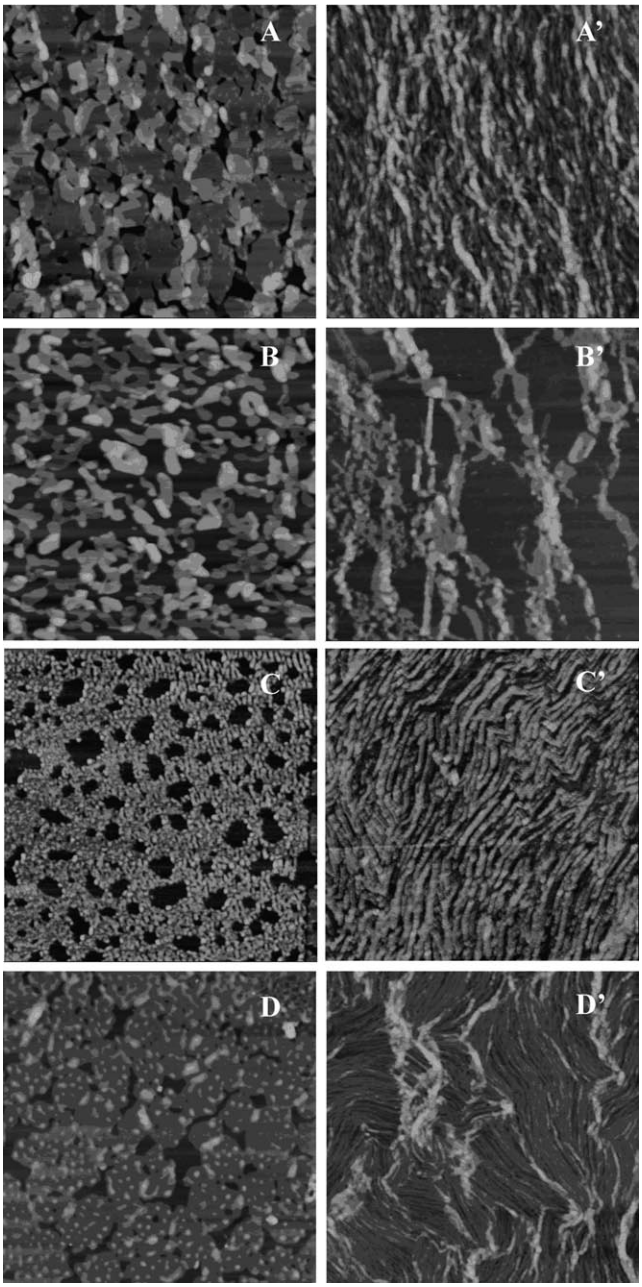

Figure 9. AFM images of monolayer LS films of the other four tetraphenylporphyrins. A, B, C, and D) Deposited from pure Milli-Q subphase; A′, B′, C′, and D′) deposited from hydrochloric acid subphase; A and A′) H_2TPPOMe; B and B′) H_2TPP; C and C′) H_2TPPOA; D and D′) H_2TPPDOMe. The scan area was $2\times2\ \mu m^2$ for all the cases. All the LS films were deposited at $30\ mN\,m^{-1}$.

shown in Figure 10. It can be seen that the maximum magnitude of the g factor at the Soret band for H_2TPPMe is 0.0031. Interestingly, the maximum magnitude of the g factor at the Soret band seems to increase with the increase of the size and/or number of the substituents on the *meso*-phenyl moiety, for all of the five investigated tetraphenylporphyrins (Table 1). For example, the LS film of H_2TPP exhibited the smallest g factor value, and those of H_2TPPMe, H_2TPPOA, and H_2TPPOMe showed moderate g factor mag-

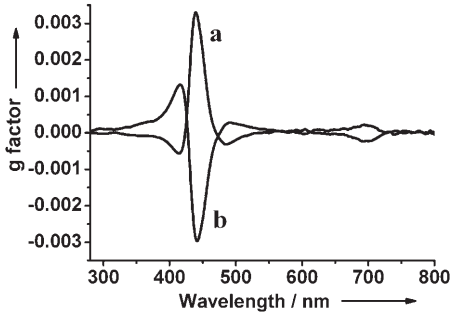

Figure 10. The g factor spectra of the LS films of the H_2TPPMe deposited from hydrochloric acid subphase. Curves a) and b) correspond to the LS films deposited in different batches.

nitudes with an approximately increasing trend, whereas that of H_2TPPDOMe displayed the largest g factor value. Thus it is reasonable to suggest that the significant steric hindrance resulting from the larger substituents on the *meso*-phenyl group could promote the occurrence of the symmetry breaking during the interfacial assembly process, because it could provide additional interspaces and degrees of freedom for the neighboring molecules in the aggregate to cooperatively stagger each other along the axis of the aggregation, producing much greater amounts of optically active supramolecules with a helical-sense conformation.

Conclusion

We have proposed a facile and general way to fabricate the optically active supramolecular assemblies from achiral porphyrins through air–water interfacial organization. The method involves the in situ diprotonation of the porphyrins at the air–dilute aqueous hydrochloric acid solution interface and subsequent formation of the LS films. The steric hindrance, partially attributed to the axial hydrogen-bonded chloride ions attached on both sides of the porphyrin plane, and partially attributed to the nonideal planarity of the porphyrin core, which resulted from the diprotonation, weakened the intermolecular π–π stacking to some extent and provided more opportunities for symmetry breaking to occur. The size and/or number of the substituents on the *meso*-phenyl moiety of the tetraphenylporphyrin appear to have some influence on the optical activities of the formulated LS films. The method is effective for all the water-insoluble free-base porphyrins we have investigated and is expected to be applicable to other porphyrin derivatives.

Experimental Section

Materials: Porphyrin derivatives, 2,3,7,8,12,13,17,18-octaethyl-21*H*,23*H*-porphine (H_2OEP, Aldrich, 97%), 5,10,15,20-tetra-*p*-tolyl-21*H*,23*H*-porphine (H_2TPPMe, Aldrich, 97%), 5,10,15,20-tetrakis(4-methoxyphenyl)-21*H*,23*H*-porphine (H_2TPPOMe, Aldrich, 95%), 5,10,15,20-tetraphenyl-21*H*,23*H*-porphine (H_2TPP, Aldrich, 99%), 5,10,15,20-tetrakis(4-(allyloxy)-phenyl)-21*H*,23*H*-porphine (H_2TPPOA, Aldrich, 98%), and 5,10,15,20-

tetrakis(3,5-dimethoxyphenyl)-21*H*,23*H*-porphine (H_2TPPDOMe, TCI, 95%), were used as received without further purification. Concentrated hydrochloric acid (HCl) was purchased from Beijing Yili Fine Chemical Co., Ltd. and diluted to 2.4 M before use as the subphase.

Procedures: The floating films on water and/or diluted (2.4 M) hydrochloric acid subphases were produced by spreading solutions of the investigated porphyrin derivatives (5×10^{-5} mol L^{-1}) in chloroform onto the surface of the pure Milli-Q water (18 MΩ cm) and/or the 2.4 M hydrochloric acid subphases, respectively. The concentration of the diluted hydrochloric acid was set at 2.4 M, because when more diluted hydrochloric acid was used (< 2.4 M), not all the porphyrin species in the LS film could be properly diprotonated. Surface pressure–area (π–A) isotherms in each case were recorded by using a KSV (KSV 1100, Finland) instrument with a compressing speed of 5 mm min^{-1} after waiting for 20 min for the chloroform solvent to evaporate. For the fabrication of the multilayer LS films of the porphyrin derivatives, the floating films were transferred onto the required solid supports at 7 mN m^{-1} (for OEP) and at 30 mN m^{-1} (for the other five porphyrin derivatives) by a horizontal lifting method by using the KSV 1100 LB apparatus. Hydrophobic quartz and hydrophobic single-face-polished silicon wafers were used as the solid supports for UV/Vis and/or CD spectra measurements, and for AFM, respectively. Samples fabricated in this way were then subjected to UV/Vis, CD, and AFM measurements. For parallel experiments, the 20-layer LS films fabricated by using the pure Milli-Q water as the subphase, were placed above the concentrated hydrochloric acid solution for about 10 min, after which the samples were subjected to the UV/Vis spectral measurement to confirm the successful diprotonation of the porphyrin species in the multilayer LS films. Then the prepared samples were also subjected to the above-mentioned measurements. To obtain acidified solutions of the compound in chloroform, a glass capillary was kept in concentrated hydrochloric acid solution for about two minutes, then the glass capillary was drawn out and immediately immersed in 1 mL of the newly prepared solutions of the porphyrin derivatives in chloroform. After magnetic stirring for 1 min, the solutions were subjected to UV/Vis and CD spectra measurements. To produce the g factor spectrum,[26] CD data was converted to delta OD (optical density) (Processing→CD options→Optical Constant) and voltage data was converted to UV/Vis absorbance (Processing→CD options→"HT→OD") by using the Spectra Analysis software. Then the g value calculation function that is incorporated in the Jasco software was used to determine the g factor spectrum by dividing the delta OD by UV/Vis absorbance.

Apparatus and the corresponding measurements: JASCO UV-550 and JASCO J-810 CD spectropolarimeters were used for the UV/Vis and CD spectral measurements, respectively. For the measurement of the CD spectra, the samples were placed perpendicular to the light path and rotated within the film plane to avoid the polarization-dependent reflections and eliminate the possible angle dependence of the CD signal.[10,11,21] The AFM height images without any image processing except flattening were recorded on a Digital Instrument Nanoscope IIIa Multimode system (Santa Barbara, CA) with a silicon cantilever by using the tapping mode.

Acknowledgements

This work was financially supported by the National Research Fund for Fundamental Key Project 973 (No. 2007CB808005 and No. 2006CB932101), National Natural Science Foundation of China (Nos. 20533050, 20773141, 20403023), and the Fund of the Chinese Academy of Sciences.

[1] a) N. Berova, K. Nakanishi, R. W. Woody, *Circular Dichroism Principles and Applications*, 2nd ed., Wiley-VCH, New York, **2000**; b) C. Branden, J. Tooze, *Introduction to Protein Structure*, 2nd ed., Garland Publishing, New York, **1999**; c) D. Voet, J. G. Voet, C. W. Pratt, *Fundamentals of Biochemistry*, Wiley, New York, **1999**; d) D. Clines, *The Physical Origin of Homochirality in Life*, AIP Press, Woodbury, New York, **1996**.

[2] a) J. J. L. M. Cornelissen, A. E. Rowan, R. J. M. Nolte, N. A. J. M. Sommerdijk, *Chem. Rev.* **2001**, *101*, 4039–4070; b) R. P. Cheng, S. H. Gellman, W. F. DeGrado, *Chem. Rev.* **2001**, *101*, 3219–3232; c) D. J. Hill, M. J. Mio, R. B. Prince, T. S. Hughes, J. S. Moore, *Chem. Rev.* **2001**, *101*, 3893–4011; d) D. B. Amabilino, J. F. Stoddart, *Chem. Rev.* **1995**, *95*, 2725–2828; e) Y. Okamoto, T. Nakano, *Chem. Rev.* **1994**, *94*, 349–372; f) T. Nakano, Y. Okamoto, *Chem. Rev.* **2001**, *101*, 4013–4038; g) L. Brunsveld, B. J. B. Folmer, E. W. Meijer, R. P. Sijbesma, *Chem. Rev.* **2001**, *101*, 4071–4097; h) R. A. Van Delden, M. K. J. Ter Wiel, M. M. Pollard, J. Vicario, N. Koumura, B. L. Feringa, *Nature* **2005**, *437*, 1337–1340; i) S. P. Fletcher, F. Dumur, M. M. Pollard, B. L. Feringa, *Science* **2005**, *310*, 80–82.

[3] a) G. Pescitelli, S. Gabriel, Y. Wang, J. Fleischhauer, R. W. Woody, N. Berova, *J. Am. Chem. Soc.* **2003**, *125*, 7613–7628; b) V. V. Borovkov, G. A. Hembury, N. Yamamoto, Y. Inoue, *J. Phys. Chem. A* **2003**, *107*, 8677–8686; c) G. Proni, G. Pescitelli, X. Huang, K. Nakanishi, N. Berova, *J. Am. Chem. Soc.* **2003**, *125*, 12914–12927; d) V. V. Borovkov, T. Harada, G. A. Hembury, Y. Inoue, R. Kuroda, *Angew. Chem.* **2003**, *115*, 1788–1791; *Angew. Chem. Int. Ed.* **2003**, *42*, 1746–1749; e) Y. Koto, T. Ohno, J.-I. Yamanaka, S. Tokita, T. Iida, Y. Ishimaru, *J. Am. Chem. Soc.* **2001**, *123*, 12700–12701; f) V. V. Borovkov, J. M. Lintuluoto, H. Sugeta, M. Fujiki, R. Arakawa, Y. Inoue, *J. Am. Chem. Soc.* **2002**, *124*, 2993–3006; g) J. M. Lintuluoto, V. V. Borovkov, Y. Inoue, *J. Am. Chem. Soc.* **2002**, *124*, 13676–13677; h) V. V. Borovkov, J. M. Lintuluoto, M. Sugiura, Y. Inoue, R. Kuroda, *J. Am. Chem. Soc.* **2002**, *124*, 11282–11283; i) V. V. Borovkov, G. A. Hembury, Y. Inoue, *Angew. Chem.* **2003**, *115*, 5468–5472; *Angew. Chem. Int. Ed.* **2003**, *42*, 5310–5314; j) T. Kurtán, N. Nesnas, F. E. Koehn, Y.-O. Li, K. Nakanishi, N. Berova, *J. Am. Chem. Soc.* **2001**, *123*, 5974–5982; k) V. V. Borovkov, G. A. Hembury, Y. Inoue, *J. Org. Chem.* **2005**, *70*, 8743–8754.

[4] a) N. Solladié, N. Aubert, J.-P. Gisselbrecht, M. Gross, C. Sooambar, V. Troiani, *Chirality* **2003**, *15*, S50–S56; b) P. A. J. De Witte, M. Castriciano, J. L. M. Cornelissen, L. M. Scolaro, R. J. M. Nolte, A. E. Rowan, *Chem. Eur. J.* **2003**, *9*, 1775–1781; c) M. Balaz, J. D. Steinkruger, G. A. Ellestad, N. Berova, *Org. Lett.* **2005**, *7*, 5613–5616; d) D. Monti, M. Venanzi, G. Mancini, C. D. Natalec, R. Paolesseac, *Chem. Commun.* **2005**, 2471–2473.

[5] a) V. V. Borovkov, J. M. Lintuluoto, Y. Inoue, *J. Am. Chem. Soc.* **2001**, *123*, 2979–2989; b) A. Mammana, M. De. Napoli, R. Lauceri, R. Purrello, *Bioorg. Med. Chem.* **2005**, *13*, 5159–5163; c) V. V. Borovkov, J. M. Lintuluoto, M. Fujiki, Y. Inoue, *J. Am. Chem. Soc.* **2000**, *122*, 4403–4407; d) L. M. Scolaro, A. Romeo, R. F. Pasternack, *J. Am. Chem. Soc.* **2004**, *126*, 7178–7179; e) M. Ayebe, K. Yamashita, K. Sada, S. Shinka, A. Ikeda, S. Sakamoto, K. Yamaguchi, *J. Org. Chem.* **2003**, *68*, 1059–1066; f) Y. Ferrand, P. L. Maux, G. Simonneaux, *Org. Lett.* **2004**, *6*, 3211–3214; g) C.-M. Che, J.-S. Huang, F.-W. Lee, Y. Li, T.-S. Lai, H.-L. Kwong, P.-F. Teng, W.-S. Lee, W.-C. Lo, S.-C. Peng, Z.-Y. Zhou, *J. Am. Chem. Soc.* **2001**, *123*, 4119–4129; h) H.-Y. Liu, J.-W. Huang, X. Tian, X.-D. Jiao, G.-T. Luo, L.-N. Ji, *Chem. Commun.* **1997**, *16*, 1575–1576; i) H.-Y. Liu, J.-C. Tian, Y. Xiao, Z.-G. Xu, S.-J. Liao, C.-K. Chang, *Chinese J. Struct. Chem.* **2005**, *24*, 263–268.

[6] a) J. Tabei, M. Shiotsuki, F. Sanda, T. Masuda, *Macromolecules* **2005**, *38*, 9448–9454; b) T. Ema, N. Ouchi, T. Doi, T. Korenaga, T. Sakai, *Org. Lett.* **2005**, *7*, 3985–3988; c) H. Nakagawa, T. Nagano, T. Higuchi, *Org. Lett.* **2001**, *3*, 1805–1807.

[7] a) R. Lauceri, A. Raudino, L. M. Scolaro, N. Micali, R. Purrello, *J. Am. Chem. Soc.* **2002**, *124*, 894–895; b) R. Purrello, A. Aaudino, L. M. Scolaro, A. Loisi, E. Bellacchio, R. Lauceri, *J. Phys. Chem. B* **2000**, *104*, 10900–10908; c) L. Zhang, J. Yuan, M. Liu, *J. Phys. Chem. B* **2003**, *107*, 12768–12773; d) S. Jiang, M. Liu, *J. Phys. Chem. B* **2004**, *108*, 2880–2884; e) J. Lang, M. Liu, *J. Phys. Chem. B* **1999**, *103*, 11393–11397; f) X. Chen, M. Liu, *J. Inorg. Biochem.* **2003**, *94*, 106–113; g) H. Onouchi, T. Miyagawa, K. Morino, E. Yashima, *Angew. Chem.* **2006**, *118*, 2441–2444; *Angew. Chem. Int. Ed.* **2006**, *45*, 2381–2384; h) J.-L. Hou, H.-P. Yi, X.-B. Shao, C. Li, Z.-Q.

Wu, X.-K. Jiang, L.-Z. Wu, C.-H. Tung, Z.-T. Li, *Angew. Chem.* **2006**, *118*, 810–814; *Angew. Chem. Int. Ed.* **2006**, *45*, 796–800.

[8] a) J. M. Ribó, J. Crusats, F. Sagués, J. Claret, R. Rubires, *Science* **2001**, *292*, 2063–2066; b) R. Rubires, J.-A. Farrera, J. M. Ribó, *Chem. Eur. J.* **2001**, *7*, 436–446; c) C. Escudero, J. Crusats, I. Díez-Pérez, Z. El-Hachemi, J. M. Ribó, *Angew. Chem.* **2006**, *118*, 8200–8203; *Angew. Chem. Int. Ed.* **2006**, *45*, 8032–8035.

[9] T. Yamaguchi, T. Kimura, H. Matsuda, T. Aida, *Angew. Chem.* **2004**, *116*, 6510–6515; *Angew. Chem. Int. Ed.* **2004**, *43*, 6350–6355.

[10] a) P. Chen, X. Ma, P. Duan, M. Liu, *ChemPhysChem* **2006**, *7*, 2419–2423; b) L. Zhang, M. Liu, *J. Phys. Chem. B* **2003**, *107*, 2565–2569; c) X. Zhai, L. Zhang, M. Liu, *J. Phys. Chem. B* **2004**, *108*, 7180–7185.

[11] a) J. Yuan, M. Liu, *J. Am. Chem. Soc.* **2003**, *125*, 5051–5056; b) X. Huang, C. Li, S. Jiang, X. Wang, B. Zhang, M. Liu, *J. Am. Chem. Soc.* **2004**, *126*, 1322–1323.

[12] The concentration of the diluted hydrochloric acid was set as 2.4 M, because when more diluted hydrochloric acid was used (< 2.4 M), not all the porphyrin species in the LS film could be properly diprotonated.

[13] a) V. S. Chirvony, A. V. Hoek, V. A. Galievsky, I. V. Sazanovich, T. J. Schaafsma, D. Holten, *J. Phys. Chem. B* **2000**, *104*, 9909–9917; b) A. Rosa, G. Ricciardi, E. J. Baerends, A. Romeo, L. M. Scolaro, *J. Phys. Chem. A* **2003**, *107*, 11468–11482.

[14] a) I. H. Wasbotten, J. Conradie, A. Ghosh, *J. Phys. Chem. B* **2003**, *107*, 3613–3623; b) B. Cheng, O. Q. Munro, H. M. Marques, W. R. Scheidt, *J. Am. Chem. Soc.* **1997**, *119*, 10732–10742.

[15] a) J. R. Weinkauf, S. W. Cooper, A. Schweiger, C. C. Wamser, *J. Phys. Chem. A* **2003**, *107*, 3486–3496; b) E. C. A. Ojadi, H. Linschitz, M. Gouterman, R. I. Walter, J. S. Lindsey, R. W. Wagner, P. R. Droupadi, W. Wang, *J. Chem. Phys.* **1993**, *97*, 13192–13197.

[16] a) G. De Luca, G. Pollicino, A. Romeo, L. M. Scolaro, *Chem. Mater.* **2006**, *18*, 2005–2007; b) G. De Luca, A. Romeo, L. M. Scolaro, *J. Phys. Chem. B* **2006**, *110*, 14135–14141.

[17] a) S. Okada, H. Segawa, *J. Am. Chem. Soc.* **2003**, *125*, 2792–2796; b) D. L. Akins, H.-R. Zhu, C. Guo, *J. Phys. Chem.* **1996**, *100*, 5420–5425.

[18] a) M. Kasha, H. R. Rawls, M. Ashraf El-Bayoumi, *Pure Appl. Chem.* **1965**, *11*, 371–392; b) E. G. McRae, M. Kasha, *J. Chem. Phys.* **1958**, *28*, 271–277.

[19] a) R. Viswanathan, J. A. Zasadzinski, D. K. Schwartz, *Nature* **1994**, *368*, 440–443; b) E. Yashima, K. Maeda, Y. Okamoto, *Nature* **1999**, *399*, 449–451.

[20] a) H. G. Kuball, T. Höfer, *Chirality* **2000**, *12*, 278–286; b) R. Kuroda, T. Harada, Y. Shindo, *Rev. Sci. Instrum.* **2001**, *72*, 3802–3810; c) J. Frelek, W. J. Szczepek, S. Neubrech, B. Schultheis, J. Brechtel, H. G. Kuball, *Chem. Eur. J.* **2002**, *8*, 1899–1907.

[21] C. Spitz, S. Dähne, A. Ouart, H. W. Abraham, *J. Phys. Chem. B* **2000**, *104*, 8664–8669.

[22] a) H. Engelkamp, S. Middelbeek, R. J. M. Nolte, *Science* **1999**, *284*, 785–788; b) P. Chen, X. Ma, M. Liu, *Macromolecules* **2007**, *40*, 4780–4784.

[23] W. R. Scheidt, I. Turowska-Tyrkl, *Inorg. Chem.* **1994**, *33*, 1314–1318.

[24] D. C. Barber, R. A. Freitag-Beeston, D. G. Whitten, *J. Phys. Chem.* **1991**, *95*, 4074–4086.

[25] Y. Zhang, M. X. Li, M. Y. Lü, R. H. Yang, F. Liu, K. A. Li, *J. Phys. Chem. A* **2005**, *109*, 7442–7448.

[26] a) P. McPhie, *Biopolymers* **2004**, *75*, 140–147; b) P. McPhie, *Anal. Biochem.* **2001**, *293*, 109–119.

Received: August 27, 2007
Published online: December 6, 2007

